CrossMark

THE JOURNAL OF NAVIGATION (2020), **73**, 1358–1371. © The Royal Institute of Navigation 2020
doi:10.1017/S0373463320000338

Research on Real-Time Obstacle Avoidance Planning for an Unmanned Surface Vessel based on the Grid Cell Mechanism

Yun Li[1] and Jian Zheng[2]

[1](*Merchant Marine College, Shanghai Maritime University, 201306 Shanghai, China*)
[2](*Transport and Communications College, Shanghai Maritime University, 201306 Shanghai, China*)
(E-mail: 1027046594@qq.com)

Obstacle avoidance navigation for an unmanned surface vessel is a research focus for ship autonomy in which the real-time requirement in practical application is very serious, and always necessitates a complicated structure model to guarantee real-time performance. This paper proposes the grid cell activation model to reduce the complexity of modelling and to simplify an obstacle avoidance algorithm. Combined with the goal-oriented probability model to design a dynamic positive-loss-rate expectation evaluation function, it produces the proper strategy for obstacle avoidance. Case studies on multi-obstacle layouts and special circumstances are conducted and presented. The results indicate that the grid cell obstacle avoidance algorithm can effectively implement obstacle avoidance planning and ensure real-time requirements. A comparison with the potential field algorithm is performed, which shows good results and verifies the feasibility of the algorithm.

KEYWORDS

1. Real-Time Obstacle Avoidance. 2. Grid Cell. 3. Goal-Oriented. 4. Unmanned Surface Vessel.

Submitted: 29 October 2019. Accepted: 6 June 2020. First published online: 3 July 2020.

1. INTRODUCTION. With the development of intelligent technology, the application of unmanned surface vessels (USVs) in ocean surveying, rescue, patrol and other fields has become more and more extensive, and the related research is becoming more and more mature, mainly focusing on unmanned vessel control, tracking navigation, obstacle avoidance navigation, formation navigation and so on. Thus, at present, obstacle avoidance is one of the most important problems in research. Obstacle avoidance navigation is also, in essence, a path selection problem, and the goal of solving the problem is to realise the optimal obstacle avoidance path at the least cost. So, according to the different levels of understanding of the environment, obstacle avoidance planning can be divided into two types: global planning and local planning.

https://doi.org/10.1017/S0373463320000338 Published online by Cambridge University Press

Global planning involves finding the appropriate path from the starting point to the final point according to a certain search algorithm after fully grasping the environmental information. The common methods are the visual graph method, probabilistic path map method, grid method and so on (Hong and Park, 2011; Yao et al., 2017), which are usually used to construct an obstacle avoidance plan with the obstacle layout being obtained in advance. Considering the rules of collision avoidance at sea, Naeem et al. (2012) set up the geometric region to divide the obstacle avoidance zone by using global map planning. The improved A* algorithm was used to carry out the obstacle avoidance planning of USV. In Sun (2018), the improved A* algorithm and the potential field grid method were combined to develop a two-level global programming algorithm to obtain the optimal path, with the dual aims of effective obstacle avoidance and shorter voyage distance. Sun (2017) adopted the global path planning algorithm based on the multi-class classification support vector machine (SVM), which independently selected the parameter indices of path smoothness and obstacle distance in each bisector, and combined them with the kernel function method to complete path planning based on the binary SVM. Zhang (2008) designed the global path planning of a USV using a genetic algorithm and artificial potential field method, which can plan for a variety of complex obstacle environments, and has the ability to find the optimal path in a three-sided obstacle environment around the starting point. Shi et al. (2018) used satellite remote sensing imagery to monitor the obstacle map, and then applied graph theory to plan the path. Wang et al. (2019) improved the wolf swarm algorithm to optimise the maximum expected programming function and obtained the optimal obstacle avoidance path.

However, global planning is not suitable for dealing with dynamic or sudden obstacle targets, and it needs to obtain enough environmental information to predict the next action (Zhu and Zhong, 2010; Raja and Pugazhenthi, 2012; González et al., 2016). In fact, it is often faced with an unknown unstructured environment. The difficulties of obstacle avoidance navigation are strengthened due to the (in)ability to acquire environmental information and real-time requirements. Therefore, local planning has become the primary choice for autonomous obstacle avoidance navigation, and the corresponding real-time obstacle avoidance model has also been developed. Some research focuses on the establishment of a geometric region model to obtain an obstacle avoidance model. For unknown obstacle information, Wu et al. (2014) considered the influence of wind and current on the manoeuvring characteristics of an unmanned aerial vehicle (UAV), analysed the model of relative velocity and relative position between UAV and obstacle, and realised the avoidance of a dynamic obstacle through change in the direction of movement. Zhu et al. (2016) proposed a constraint reference frame to develop the potential field so that the decomposed forces can be matched with the physical constraints of the UAV for online adjustment. Pu et al. (2017) put forward a predictable dynamic obstacle avoidance method for an unmanned submarine based on collision cone deduction, calculated the collision angle region for collision between an unmanned submarine and a dynamic obstacle, and obtained the collision angle of an unmanned submarine. Qu et al. (2013) used the combination of a genetic algorithm and a geometric region obstacle avoidance model to design an obstacle avoidance strategy. Chen et al. (2018) designed a discrete-time nonlinear velocity obstacle avoidance method to predict the state of obstacle avoidance for a dynamic obstacle. Combined with devising collision avoidance rules, collision avoidance planning in a multi-obstacle environment was carried out and the idea of tracking was introduced into obstacle avoidance in Zhang et al. (2018). Song et al. (2018) divided the problem of dynamic target obstacle avoidance

https://doi.org/10.1017/S0373463320000338 Published online by Cambridge University Press

planning into two levels, the first of which used the speed obstacle avoidance algorithm, and the second established the improved artificial potential field algorithm. The two levels were combined to adjust the speed and direction of the unmanned vessel. A proper penalty function field has been proposed in Lee et al. (2018) to be optimal collision-free transfers in real time, improving the efficiency of the obstacle avoidance model.

Some workers have paid attention to adaptive prediction and feedback learning for enhancing the performance of obstacle avoidance. Zhao et al. (2016) used a neural network to design a collision avoidance model for evaluating the collision situation. The work of Kozynchenkoa and Kozynchenko (2018) was specially designed for a ships crossing scenario using dynamic predictive programming based on a neural network and fuzzy algorithm. Zhang et al. (2014) proposed an adaptive risk aversion decision model using the Sarsa (state–action–reward–state–action) online strategy reinforcement learning algorithm, and combined this with a progressive corruption algorithm as a behaviour exploration strategy. Wang et al. (2018) established a Markov decision-making method through reinforcement learning, and then the optimal strategy was solved by value function programming and simulated in static and dynamic obstacle environments. The deep reinforcement learning was also applied to train ships to avoid obstacles automatically (Shen et al., 2019).

At present, from the simple geometric collision region determination model to the nonlinear uncertainty prediction model, from offline learning to online real-time learning, most research increases the structure and judgment complexity of an obstacle avoidance algorithm or model in order to ensure the real-time performance of obstacle avoidance. Therefore, this paper considers reducing the complexity of the obstacle avoidance strategy model, to design a new obstacle avoidance algorithm for ensuring real-time requirements and simplifying the processing model, which can achieve the purpose of autonomous obstacle avoidance. This approach is believed to have the following advantages over existing solutions: (1) The grid cell activation model is constructed by using the bio-grid cell heuristic algorithm to simplify the model describing the distance relationship between the USV and the obstacle. (2) Considering the uncertainty, the dynamic expectation evaluation function is designed from the viewpoint of probability, which refers to the target orientation and decreases the spatial execution dimension, especially in the face of an unknown and complex environment.

The rest of the paper is organised as follows. In Section 2, the problem description is given. Section 3 presents the detailed design algorithm for obstacle avoidance. Simulation experiments under different obstacle scenarios are given in Section 4. Finally, the paper concludes in Section 5.

2. PROBLEM DESCRIPTION.

We consider that a USV will sail to designated target locations in multi-obstacle unknown environments, focusing on two main areas: (1) acquisition of environmental information, and (2) goal-oriented obstacle avoidance planning. Owing to the fact that this is real-time obstacle avoidance in the face of a locally known situation, it is not necessary to know all the environmental information, but only to make judgments on the basis of the information obtained from the actual sensors, and to establish a model to describe the distance between the USV and the obstacle. In order to reduce the complexity of the model, the grid cell activation model in bionics is combined to simplify the obstacle avoidance model. Meanwhile, aiming at the specified target location,

https://doi.org/10.1017/S0373463320000338 Published online by Cambridge University Press

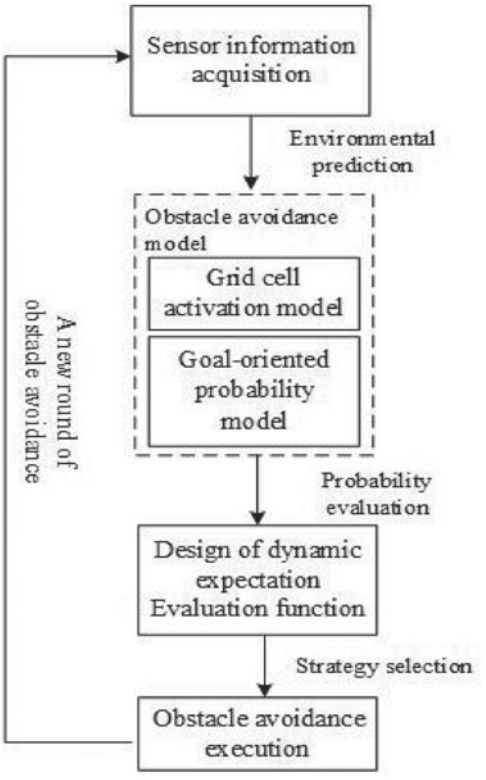


Figure 1. Overall process of the obstacle avoidance algorithm.

the dynamic expectation evaluation function, including reward and punishment factors, is constructed to evaluate the optimal obstacle avoidance decision, through a design initialisation and update strategy, to reduce the judgment dimension, and to quickly obtain the execution decision for guaranteeing the real-time requirement. The overall process is shown in Figure 1.

3. DESIGN OF OBSTACLE AVOIDANCE ALGORITHM.

3.1. *The grid cell activation model.* A large number of neurophysiological studies (O'Keefe and Nadel, 1978; David and Pierre, 2006; van Strien et al., 2009) have shown that, in animals, the hippocampal formation in the brain is the part of the body mainly responsible for environmental cognition. Animals are able to use self-motion cues to maintain vector relationships relative to environmentally important positions, and to compute and integrate the information of each site in space so that this vector relationship is constantly updated. This process is dominated by grid cells in the entorhinal cortex of the hippocampus (Solstad et al., 2006; Witter and Moser, 2006). Through the external discharge of the grid cells, the brain can continuously integrate the space angle and linear distance to locate the coordinates of its own environment for understanding its specific position in its surroundings. At present, the grid cell model theory is mostly used in autonomous positioning (Wei and Loo, 2018; Yu et al., 2018) and position navigation (Antonelo et al.,

https://doi.org/10.1017/S0373463320000338 Published online by Cambridge University Press

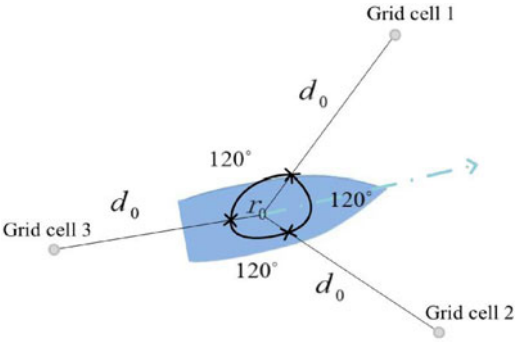


Figure 2. Grid cell structure model.

2007; Zhou and Wu, 2017). So, here, we use the grid cell model to describe the distance correlation between a USV and obstacles, and to establish the relevant regional model for obstacle avoidance.

According to Yu et al. (2016), biological studies confirmed that the grid cell fields are distributed in a triangular structure, and each grid field uses three striped cells to design the discharge activity of the grid cells. Therefore, a grid cell model based on striped cells is constructed as follows.

In Figure 2, a triangular obstacle avoidance model regarding grid cells is constructed by choosing the angles of 60°, 180° and 300° clockwise along the heading direction and extending distance d_0 from the centre of the USV, instead of paying attention to all the ship perimeter information from the perspective of 360°. The triangular endpoint formed by the extension end is thought of as the grid cell, while the USV is in a position where it needs to be activated by its discharge. Viewing the grid cell activation model, the activation function of a single grid cell can be expressed as

$$g(r) = \tfrac{2}{3}(\phi(r) + \tfrac{1}{2}), \tag{1}$$

where $\phi(r) = \frac{1}{3}\sum_i \cos(k_i(r - r_0))$ represents the discharge activity of each grid cell, r is the position of the triangle endpoint (as shown by the small circle in Figure 2), which is determined by the detected distance between the obstacle and the USV along the direction of each grid cell, and $r_0 = (x, y)$ is the position of the USV. Each grid cell is superimposed by three stripes with a difference of 60° in the direction of the wavevector, where i represents the number of the wavevector ($i = 1, 2, 3$) and k_i represents the wavevector, as follows: (2).

$$\begin{cases} k_1 = \dfrac{4\pi}{\sqrt{6}\lambda}[\cos(\theta) + \sin(\theta),\ \cos(\theta) - \sin(\theta)], \\ k_2 = \dfrac{4\pi}{\sqrt{6}\lambda}\left[\cos\left(\theta + \dfrac{\pi}{3}\right) + \sin\left(\theta + \dfrac{\pi}{3}\right),\ \cos\left(\theta + \dfrac{\pi}{3}\right) - \sin\left(\theta + \dfrac{\pi}{3}\right)\right], \\ k_3 = \dfrac{4\pi}{\sqrt{6}\lambda}\left[\cos\left(\theta + \dfrac{2\pi}{3}\right) + \sin\left(\theta + \dfrac{2\pi}{3}\right),\ \cos\left(\theta + \dfrac{2\pi}{3}\right) - \sin\left(\theta + \dfrac{2\pi}{3}\right)\right], \end{cases} \tag{2}$$

where λ is the spacing between grid cells, and θ is the course of the USV.

https://doi.org/10.1017/S0373463320000338 Published online by Cambridge University Press

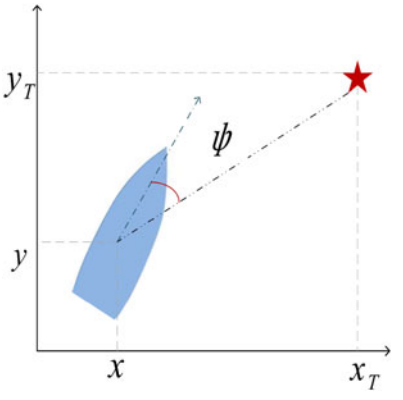


Figure 3. Goal-oriented structural model.

For the grid cell activation model in Figure 2, which consists of three grid cells, the corresponding total activation probability function is

$$p_c(r) = \sum_{1}^{N} \omega_n g(r_n). \tag{3}$$

Here N is the total number of grid cells ($n = 1, 2, \ldots, N$); $g(r_n)$ represents the activation rate of the nth grid cell at the spatial location (x, y) in the environment facing obstacles, whose function is Equation (1); and ω_n represents the connection weight between the *nth* grid cell and the discharge activation position, that is, the associated weight between the triangular endpoint formed by the extension end and the position of the USV (as shown in Figure 2), as follows:

$$\omega_n = \frac{4\pi\sigma^2}{3\lambda^2} \exp^{-4\sigma^2\pi^2/3\lambda^2}, \tag{4}$$

with σ being the standard deviation parameter of the discharge activation domain.

Therefore, the grid cell activation model is employed to express the distance correlation between obstacles and the USV. The d_0 value in the structure model of Figure 2 is set as the threshold value, and the distance information obtained from the sensor is used to judge the distance relationship between the obstacles and the USV. When any of the detected distances d along the direction of the three grid cells (r also changes with it) is less than the threshold value, the activation probability function of Equation (3) is triggered and gains the activation probability.

3.2. *The goal-oriented probability model.* In order to reach the expected position as soon as possible, when planning the obstacle avoidance strategy, it should consider the expected goal-oriented path model. Here the course angle of the USV is used as a reference index to establish the goal-oriented model:

$$\psi = \theta - \arctan\left(\frac{y_T - y}{x_T - x}\right). \tag{5}$$

Equation (5) and Figure 3 are used to describe the extent to which the current course of the USV deviates from the situation of moving towards the target, where (x_T, y_T) is

https://doi.org/10.1017/S0373463320000338 Published online by Cambridge University Press

the intended target position. Then the Gaussian distribution function is used to find its probability; the maximum probability 1 means that the USV is sailing towards the expected target, indicating that the extent of deviation is 0. With the decrease of the probability, the extent of the deviation increases gradually:

$$p(\psi) = \exp\left\{-\frac{1}{2}\left[\theta - \arctan\left(\frac{y_T - y}{x_T - x}\right)\right]^2\right\}. \tag{6}$$

Therefore, choosing the obstacle avoidance strategy always takes account of the intended target, by which path redundancy can be effectively avoided.

3.3. *Dynamic expectation evaluation function.* Combined with the above-mentioned grid cell activation model and the goal-oriented probability model, the positive-loss-rate expectation evaluation function is designed to find the maximum probability value of the possible obstacle avoidance strategy, and then the strategy selection and execution are carried out.

The positive-loss-rate expectation evaluation function is established under the condition of the maximum expected profit, and consists of the following evaluation function:

$$f_{\max} = \text{correct rate} \times \text{reward factor loss rate} \times \text{punishment factor}. \tag{7}$$

The correct rate describes the probability proportion of the three grid cell directions in the grid cell activation model, which is expressed by $(p_{c1}/p_{cm},\ p_{c2}/p_{cm},\ p_{c3}/p_{cm})$, where (p_{c1}, p_{c2}, p_{c3}) are the actual activation probabilities in the three detection directions calculated by Equation (3). Here p_{cm} means that the activation probability is calculated by choosing the threshold value d_0. The correct rate decreases with the decrease of the detected distance d.

The reward factor is mainly used to express the proportional relationship between the threshold distance d_0 for triggering obstacle avoidance and the distance d actually detected. When the detected distance satisfies $d \geq d_0$, the reward factor in this direction is considered to be the largest, and 10 is selected as the standard. When the detected distance satisfies $d < d_0$, the corresponding reward factor is $(d/d_0) \times 10$; if the detected distance d is closer to d_0, the reward value is higher, otherwise it is lower. The reward factor encourages the whole model of USV to be above the threshold distance range and stay away from the obstacle area.

As for the loss rate, it mainly describes the deviation level from the expected target position during obstacle avoidance planning, which is described by the goal-oriented probability model and expressed by $1 - p(\psi)$.

The punishment factor needs to combine the current state of the USV with the state of the next obstacle avoidance selection, and describes the deviation distance caused by the expected obstacle avoidance selection, as shown in Figure 4. The punishment factor corresponds to the loss rate, when the deviation level is large. The punishment factor is high, considering the timeliness and orientation, to avoid this kind of choice as far as possible.

According to Figure 4, the result is

$$fa = |k_0 x_f - y_f + y_T - k_0 x_T| / \sqrt{k_0^2 + 1}, \tag{8}$$

where $k_0 = \frac{(y_T - y)}{(x_T - x)}(x_f, y_f)$ is the next obstacle avoidance option position of the USV.

https://doi.org/10.1017/S0373463320000338 Published online by Cambridge University Press

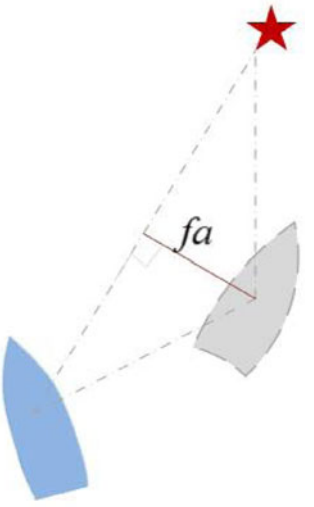


Figure 4. Schematic diagram of punishment factor.

Therefore, according to the above process, the maximum value of the expected evaluation function in Equation (7) is solved. The corresponding obstacle avoidance selection when solving the maximum expectation is executed as an actual obstacle avoidance strategy.

Moreover, in order to enhance the computational efficiency, the midline is drawn from the vertex of the triangle which is composed of the endpoints of the actual detected distance in the two detection directions of the grid cell activation model: the grid cell 1 and the grid cell 2, and the centre of the unmanned ship. The angle of transition when the current course of the USV is turned to the midline direction is taken as the adjustment angle of the initial state. Equation (9) performs a status update mode until the maximum evaluation expectation is determined:

$$\theta_{\Delta} = \beta_1 \theta + \beta_2 \arctan\left(\frac{y_T - y}{x_T - x}\right), \tag{9}$$

where β_1 and β_2 are gain parameters.

So, the obstacle avoidance algorithm has been constructed through Sections 3.1 to 3.3. It gives the optimal obstacle avoidance strategy for real-time planning. However, there is an obstacle avoidance situation that requires special treatment, referring to the following section.

3.4. *Virtual obstacle model.* What is involved above is a strategy to initiate obstacle avoidance action when the detected distance reaches the threshold distance value, but, in practice, the USV cannot be treated as a particle and needs to set up its own collision region. Once this region is entered, collision occurs, which should be avoided. For obstacle avoidance in a multi-obstacle environment, there is no way to know the global information in advance, so it is hard to predict whether it can pass safely or not. If the USV cannot pass through its own set collision region, it will choose a round-trip detour. While the USV only relies on the current situation and has no historical memory when choosing the strategy, it will cause this impassable state to happen again and again, leading to its sailing back and

https://doi.org/10.1017/S0373463320000338 Published online by Cambridge University Press

forth. Therefore, in order to break the continuous circulation of the special situation, it is necessary to add memory to the obstacle avoidance strategy, to avoid the recurrence of the previous impassable situation. In this paper, a virtual obstacle model is established to solve this kind of phenomenon.

When facing the fact that, no matter how the next strategy is chosen, the USV will finally enter its own collision area, which makes it impossible to proceed forwards and always to choose a round trip, it is necessary to take the position of the USV at that moment as the centre of a circle, to create a virtual circular obstacle of radius R and document it. Then, in the implementation of the following strategy, taking this virtual circular obstacle as an actual obstacle, it continues to deal with the judgment according to the above designed obstacle avoidance algorithm, which can avoid the occurrence of back-and-forth situations.

4. SIMULATION VERIFICATION. Here we assume that the initial position of the USV is (0, 0), the initial course is 90°, the expected target position is (50, 120), the threshold distance value is $d_0 = 10$, and the parameters are $\sigma = 0{\cdot}5$, $\beta_1 = 1$ and $\beta_2 = 0{\cdot}2$. The obstacle avoidance scene is composed of several static circular obstacles, which is simulated and demonstrated by using the MATLAB software platform.

The kinematic model is as follows:

$$\begin{cases} \dot{x} = u\cos\theta - v\sin\theta, \\ \dot{y} = u\sin\theta + v\cos\theta, \\ \dot{\theta} = r_\theta, \end{cases} \tag{10}$$

where u, v and r_θ are the velocities in the surge, sway and yaw directions, respectively. Here, any external interference is ignored, the default $v \approx 0$, and we choose $u = 2$.

4.1. *Comparative analysis of two obstacle avoidance algorithms.* According to Figure 5, the blue solid line is the algorithm designed in this paper, and the red dotted line is the obstacle avoidance planning using the artificial potential field algorithm. Through comparative analysis, it is concluded that each of the two algorithms has its own advantages and can achieve the target smoothly; the USV sails directly towards the target at the beginning, and adjusts the course angle to avoid the obstacle when encountering obstacles until it reaches the desired goal.

However, the algorithm designed in this paper is more suitable for the comprehensive evaluation of multi-obstacle environments, and is superior to the improved potential field algorithm in unknown environments. The original artificial potential field algorithm focuses on the obstacle avoidance of a single obstacle, and the planning effect does not perform well when increasing the change of obstacles layout or when the distance among obstacles becomes short. However, the new algorithm has some large turns that ensure the safety of sailing, and no closer to the obstacles than that of the original algorithm. Therefore, this proposed new algorithm can effectively achieve obstacle avoidance with good performance in the running ability and complex obstacle environment.

4.2. *Simulation of obstacle avoidance under different obstacle layouts.* According to the obstacle avoidance procedure in Section 2, the real-time obstacle avoidance strategy of the USV is carried out and verified in different obstacle position layouts. From Figures 5 and 6, it can be concluded that the USV has successfully evaded the obstacles to reach the desired position, and the trajectory is basically smooth, but, in some places, one can clearly view places with large turns. This is mainly due to the need to ensure navigation towards

https://doi.org/10.1017/S0373463320000338 Published online by Cambridge University Press

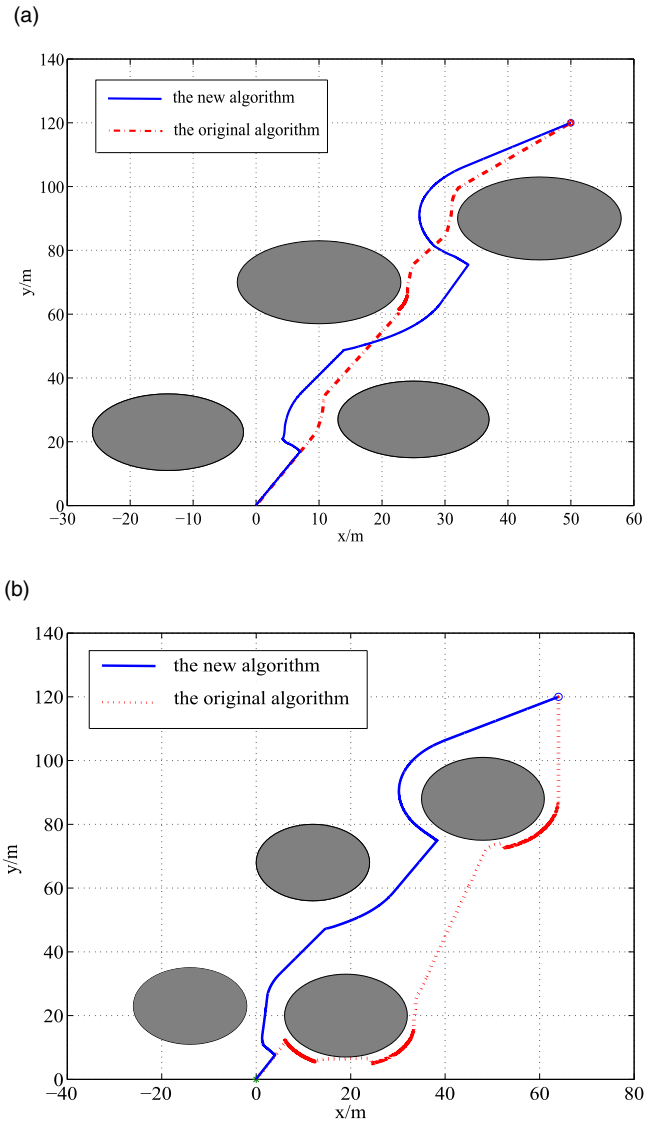


Figure 5. Effect of obstacle avoidance under two algorithms.

the target, and is also necessary to avoid collision obstacles simultaneously, resulting from their combined effect.

Compared with Figure 5, the obstacle location in Figure 6(a) is different, which results in a different path for obstacle avoidance. It selects the best strategy according to the expected maximum evaluation function, to find the appropriate way to avoid obstacles. Figure 6(b) and 6(c) are obstacle avoidance scenarios formed by decreasing and increasing the number of obstacles on the basis of Figure 6(a), respectively. Due to the difference in the number of obstacles, different obstacle avoidance paths are obtained according to the evaluation algorithm.

https://doi.org/10.1017/S0373463320000338 Published online by Cambridge University Press

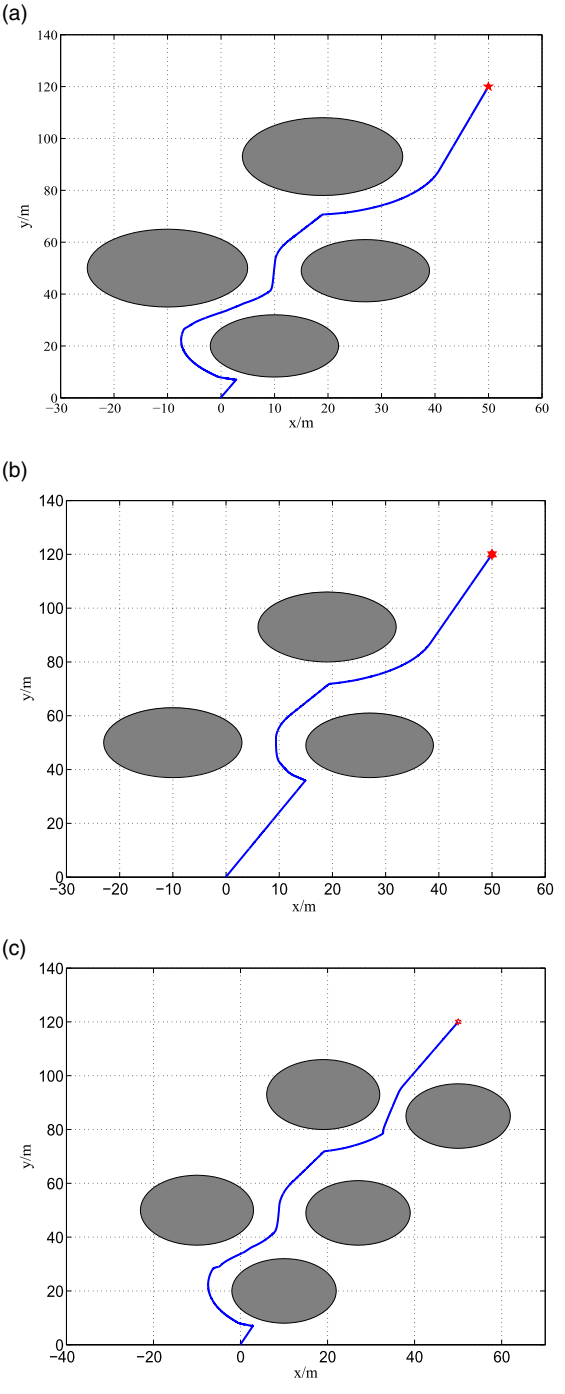


Figure 6. Effect of obstacle avoidance under different obstacle layouts.

https://doi.org/10.1017/S0373463320000338 Published online by Cambridge University Press

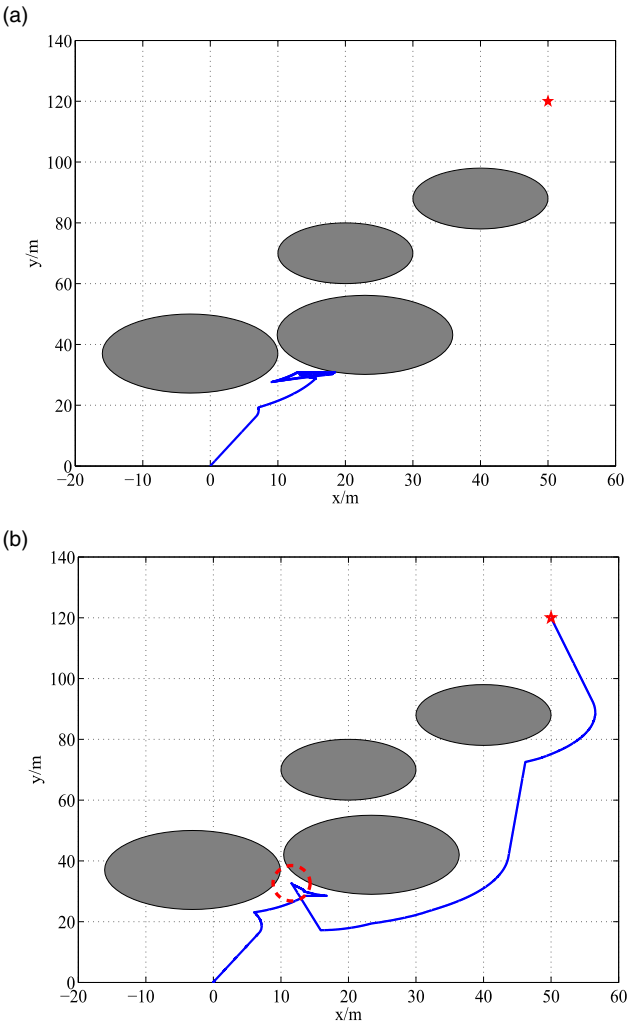


Figure 7. Effect of obstacle avoidance with and without a virtual obstacle.

In the above, the obstacle avoidance path is affected by the expected target and the number and location of obstacles encountered along the way, resulting in different planning trajectories. According to the obstacle avoidance algorithm, the decision on the surrounding obstacle environment can be made in real time, choosing the appropriate obstacle avoidance path, and successfully completing navigation to the target.

4.3. *Simulation of obstacle avoidance in the case of an impassable situation.* Under a multi-obstacle layout, for adjacent relatively close obstacles, the USV cannot pass and will choose to sail back, but due to the influence of goal guidance, it may also choose to turn back and forth again, resulting in the effect of a round trip. To avoid this particular situation, it creates a virtual obstacle model to avoid it. According to Figure 7(a), there is no virtual obstacle, causing the phenomenon of stagnating back and forth, which affects normal navigation. But the virtual obstacle avoidance model is adopted in Figure 7(b), and

https://doi.org/10.1017/S0373463320000338 Published online by Cambridge University Press

the circle represented by the red dotted line is the virtual obstacle, which is recorded as an actual obstacle, to be conducive for the later strategy choice, and the back-and-forth phenomenon is successfully avoided when encountering the round trip.

Therefore, through the above argumentation and analysis, it is shown that the real-time obstacle avoidance method designed in this paper can achieve obstacle avoidance navigation very well in the complex environment with multiple obstacles, and can also effectively avoid the special back-and-forth phenomenon.

5. CONCLUSION.

Using bionics for reference, this paper constructs an obstacle avoidance method combining the grid cell activation model and the goal-oriented probability model, and designs a positive-loss-rate expectation evaluation function to optimise the obstacle avoidance strategy, considering the reduction of execution complexity, where the structure of obstacles is ignored, and it is not necessary to know the surrounding environment information in advance. The later verification results are good, and there is a smooth and reasonable obstacle avoidance trajectory, which has a simplified structure, meets the real-time requirements and effectively solves the real-time obstacle avoidance problem in a multi-obstacle environment. However, this paper does not deal with the impact of a dynamic obstacle, and the lack of ship manoeuvrability, and, in addition, the large turns in the path should be weakened for further consideration in actual situations; it is necessary to further explore all of these in the future.

ACKNOWLEDGMENTS

This work is supported by the National Natural Science Foundation of China under Grants Nos. 51909155 and 51709166.

REFERENCES

Antonelo, E. A., Schrauwen, B. and Campenhout, J. V. (2007). Generative modeling of autonomous robots and their environments using reservoir computing. *Neural Processing Letters*, **26**, 233–249.

Chen, P., Huang, Y., Mou, J. and van Gelder, P. H. A. J. M. (2018). Ship collision candidate detection method: A velocity obstacle approach. *Ocean Engineering*, **170**, 186–198.

David, A. and Pierre, L. (2006). *Hippocampal neuroanatomy*. Oxford: Oxford University Press, 37–115.

González, D., Pérez, J., Milanés, V. and Nashashibi, F. (2016). A review of motion planning techniques for automated vehicles. *IEEE Transactions on intelligent transportation systems*, **17**(4), 1135–1145.

Hong, J. P. and Park, K. (2011). A new mobile robot navigation using a turning point searching algorithm with the consideration of obstacle avoidance. *The International Journal of Advanced Manufacturing Technology*, **52**, 763–775.

Kozynchenkoa, A. I. and Kozynchenko, S. A. (2018). Applying the dynamic predictive guidance to ship collision avoidance: Crossing case study simulation. *Ocean Engineering*, **164**, 640–649.

Lee, K., Parka, C. and Eun, Y. (2018). Real-time collision avoidance maneuvers for spacecraft proximity operations via discrete-time Hamilton–Jacobi theory. *Aerospace Science and Technology*, **77**, 688–695.

Naeem, W., Irwin, G. W. and Yang, A. (2012). COLREGs-based collision avoidance strategies for unmanned surface vehicles. *Mechatronics*, **22**, 669–678.

O'Keefe, J. and Nadel, L. (1978). The hippocampus as a cognitive map. *American Journal of Psychology*, **168**(3), 863.

Pu, H. Y., Feng, D. and Li, X. M., et al. (2017). Maritime autonomous obstacle avoidance in a dynamic environment based on collision cone of ellipse. *Chinese Journal of Scientific Instrument*, **38**(7), 1756–1762.

Qu, H., Xing, K. and Alexander, T. (2013). An improved genetic algorithm with coevolutionary strategy for global path planning of multiple mobile robots. *Neurocomputing*, **120**, 509–517.

https://doi.org/10.1017/S0373463320000338 Published online by Cambridge University Press

Raja, P. and Pugazhenthi, S. (2012). Optimal path planning of mobile robots: A review. *International Journal of the Physical Sciences*, **7**(9), 1314–1320.

Shen, H., Hashimoto, H., Matsuda, A., Taniguchi, Y., Terada, D. and Guo, C. (2019). Automatic collision avoidance of multiple ships based on deep Q-learning. *Applied Ocean Research*, **86**, 268–288.

Shi, B. H., Su, Y. X. and Zhang, H. J. (2018). Obstacles modeling method in cluttered environments using satellite images and its application to path planning for USV. *International Journal of Naval Architecture and Ocean Engineering*, **3**, 1–9.

Solstad, T., Moser, E. I. and Einevoll, G. T. (2006). From grid cells to place cells: A mathematical model. *Hippocampus*, **16**(12), 1026–1031.

Song, A. L., Su, B. Y., Dong, C. Z., Shen, D. W., Xiang, E. Z. and Mao, F. P. (2018). A two-level dynamic obstacle avoidance algorithm for unmanned surface vehicles. *Ocean Engineering*, **170**, 351–360.

Sun, Q. G. (2017). *Path planning for ship navigation based on support vector machine*. Liaoning, China: Dalian Maritime University.

Sun, Y. D. (2018). *A Research on Intelligent Planning for Ship Navigation Path*. Liaoning, China: Dalian Maritime University.

van Strien, N. M., Cappaert, N. L. and Witter, M. P. (2009). The anatomy of memory: An interactive overview of the parahippocampal-hippocampal network. *Nature Reviews Neuroscience*, **10**(4), 272–282.

Wang, C. B., Zhang, X. Y. and Zhang, J. W., et al. (2018). Method for intelligent obstacle avoidance decision-making of unmanned vessel in unknown waters. *Chinese Journal of Ship Research*, **13**(6), 72–77.

Wang, Y. Y., Yao, P. and Dou, Y. M. (2019). Monitoring trajectory optimisation for unmanned surface vessel in sailboat race. *International Journal for Light and Electron Optics*, **176**, 394–400.

Wei, H. C. and Loo, C. K. (2018). Topological Gaussian ARAM for biologically inspired topological map building. *Neural Computing and Applications*, **29**, 1055–1072.

Witter, M. P. and Moser, E. I. (2006). Spatial representation and the architecture of the entorhinal cortex. *Trends in Neurosciences*, **29**(12), 671–678.

Wu, B., Xiong, Y. and Wen, Y. Q. (2014). Automatic collision avoidance algorithm for unmanned surface vessel based on velocity obstacles. *Journal of Dalian Maritime University*, **40**(2), 13–16.

Yao, P., Wang, H. L. and Ji, H. X. (2017). Gaussian mixture model and receding horizon control for multiple UAV search in complex environment. *Nonlinear Dynamics*, **88**, 903–919.

Yu, N. G., Fang, L., Luo, Z. W., Yuan, Y., Jiang, X. and Cai, J. (2016). From grid cells to place cells: A gauss distribution activation function model. *Journal of biomedical engineering*, **33**(6), 1158–1167.

Yu, N. G., Yuan, Y. H. and Li, T., et al. (2018). A cognitive map building algorithm by means of cognitive mechanism of hippocampus. *Acta Automatica Sinica*, **44**(1), 52–73.

Zhang, Y. K. (2008). *Research on Path Planning for Unmanned Surface vehicle*. Heilongjiang, China: Harbin Engineering University.

Zhang, R., Tang, P., Su, Y., Li, X., Yang, G. and Shi, C. (2014). An adaptive obstacle avoidance algorithm for unmanned surface vehicle in complicated marine environments. *IEEE/CAA Journal of Automatica Sinica*, **1**(4), 385–396.

Zhang, G. Q., Deng, Y. J., Zhang, W. D. and Huang, C. (2018). Novel DVS guidance and path-following control for underactuated ships in presence of multiple static and moving obstacles . *Ocean Engineering*, **170**, 100–110.

Zhao, Y. X., Li, W. and Shi, P. (2016). A real-time collision avoidance learning system for Unmanned Surface Vessels. *Neurocomputing*, **182**, 255–266.

Zhou, Y. and Wu, D. W. (2017). Location estimation model based on the transformation from grid cells to place cells. *Journal of Electronics and Information Technology*, **39**(9), 2272–2276.

Zhu, D. Q. and Zhong, Y. M. (2010). Survey on technology of mobile robot path planning. *Control and Decision*, **25**(7), 961–967.

Zhu, L. H., Cheng, X. H. and Yuan, F. G. (2016). A 3D collision avoidance strategy for UAV with physical constraints. *Measurement*, **77**, 40–49.

https://doi.org/10.1017/S0373463320000338 Published online by Cambridge University Press